

Shared and Unique Functions of the DExD/H-Box Helicases RIG-I, MDA5, and LGP2 in Antiviral Innate Immunity¹

Mitsutoshi Yoneyama,* Mika Kikuchi,* Kanae Matsumoto,* Tadaatsu Imaizumi,†
Makoto Miyagishi,*§ Kazunari Taira,*¶ Eileen Foy,|| Yueh-Ming Loo,|| Michael Gale, Jr.,||
Shizuo Akira,# Shin Yonehara,** Atsushi Kato,†† and Takashi Fujita*²

The cellular protein retinoic acid-inducible gene I (RIG-I) senses intracellular viral infection and triggers a signal for innate antiviral responses including the production of type I IFN. RIG-I contains a domain that belongs to a DExD/H-box helicase family and exhibits an N-terminal caspase recruitment domain (CARD) homology. There are three genes encoding RIG-I-related proteins in human and mouse genomes. Melanoma differentiation associated gene 5 (MDA5), which consists of CARD and a helicase domain, functions as a positive regulator, similarly to RIG-I. Both proteins sense viral RNA with a helicase domain and transmit a signal downstream by CARD; thus, these proteins share overlapping functions. Another protein, LGP2, lacks the CARD homology and functions as a negative regulator by interfering with the recognition of viral RNA by RIG-I and MDA5. The nonstructural protein 3/4A protein of hepatitis C virus blocks the signaling by RIG-I and MDA5; however, the V protein of the Sendai virus selectively abrogates the MDA5 function. These results highlight ingenious mechanisms for initiating antiviral innate immune responses and the action of virus-encoded inhibitors. *The Journal of Immunology*, 2005, 175: 2851–2858.

Intracellular antiviral responses, including the activation of type I IFN genes, are initiated by the recognition of dsRNA generated by the replication of infected viruses. Type I IFN plays a critical role in initiating antiviral innate immunity and modulating subsequent adaptive immunity (1, 2). A dsRNA-induced signal is transmitted to the nucleus via a series of transcription factors, including IFN regulatory factor (IRF)³-3, IRF-7, NF- κ B, and activating transcription factor-2/c-Jun (3). Among them, IRF-3 is essential for the primary activation of IFN genes (4). IRF-3 is phosphorylated at specific serine residues (5, 6) by two

members of the I κ B kinase (IKK) family, TANK-binding kinase 1 (TBK1) and IKKi/IKK ϵ (7, 8), and forms an active DNA-binding holocomplex with a transcriptional coactivator, p300 or the CREB-binding protein, in the nucleus (9). The analysis of knockout mice for *tbk1* and *ikki* genes demonstrated the essential and redundant role of these genes in the activation of IRF-3 (10, 11). IRF-7 is also regulated by these kinases and involved in the secondary induction of IFN genes (8, 12, 13).

Recently, we have identified a DExD/H-box-containing RNA helicase, retinoic acid-inducible gene I (RIG-I), as an essential component of the sensor of intracellular dsRNA (14). RIG-I encodes a caspase recruitment domain (CARD) at the N terminus, in addition to an RNA helicase domain. The helicase domain recognizes dsRNA and regulates signal transduction in an ATPase-dependent manner. Although the CARD of RIG-I directly transmits a signal leading to the activation of both IRF-3 and NF- κ B, the precise machinery for the activation remains unknown. In the mammalian database, we found two other DExD/H-box-containing RNA helicases that are closely related to RIG-I. Melanoma differentiation-associated gene 5 (MDA5) is the closest relative of RIG-I, exhibiting 23 and 35% aa identities in the N-terminal CARD and C-terminal helicase domain, respectively. MDA5 has been implicated in the regulation of the growth and differentiation of melanoma cells (15). MDA5 was independently identified as a binding target for V proteins of paramyxoviruses (16). Although the precise mechanism is unclarified, these V proteins inhibit the dsRNA-induced activation of the IFN- β gene through MDA5. Another helicase, LGP2 (17), shows 31 and 41% aa identities to the helicase domains of RIG-I and MDA5, respectively, but completely lacks CARD. In this report, we show that MDA5 acts as a positive regulator in the virus-induced activation of type I IFN genes. We provide evidence that RIG-I and MDA5 transmit an identical signal leading to the activation of IRF-3, IRF-7, and NF- κ B. Many virus-encoded proteins specifically target these helicases to escape from antiviral detection by the host cells. The other family member LGP2 functions as a dominant-negative regulator

*Antiviral Innate Immunity Project, Tokyo Metropolitan Institute of Medical Science, Tokyo Metropolitan Organization for Medical Research, Tokyo, Japan; †Department of Vascular Biology, Hirosaki University School of Medicine, Hirosaki, Aomori, Japan; ‡21st Century Center of Excellence Program, Graduate School of Medicine, University of Tokyo, Tokyo, Japan; §National Institute of Advanced Industrial Science and Technology, Gene Function Research Center, Tsukuba Science City, Japan; ¶Department of Chemistry and Biotechnology, School of Engineering, University of Tokyo, Tokyo, Japan; ||Department of Microbiology, University of Texas Southwestern Medical Center, Dallas, TX 75390; #Department of Host Defense, Research Institute for Microbial Diseases, Osaka University, Suita, Osaka, Japan; **Department of Animal Development and Physiology, Graduate School of Biostudies, Kyoto University, Kyoto, Japan; and ††Department of Virology III, National Institute of Infectious Diseases, Musashimurayama, Tokyo, Japan

Received for publication March 11, 2005. Accepted for publication June 16, 2005.

The costs of publication of this article were defrayed in part by the payment of page charges. This article must therefore be hereby marked *advertisement* in accordance with 18 U.S.C. Section 1734 solely to indicate this fact.

¹ This work is supported by Japan Society for the Promotion of Science, Ministry of Education, Culture, Sports, Science and Technology of Japan, Nippon Boehringer Ingelheim, and Toray Industries.

² Address correspondence and reprint requests to Dr. Takashi Fujita, Antiviral Innate Immunity Project, Tokyo Metropolitan Institute of Medical Science, Tokyo Metropolitan Organization for Medical Research, 3-18-22 Honkomagome, Bunkyo-ku, Tokyo 113-8613, Japan. E-mail address: fujita@rinshoken.or.jp

³ Abbreviations used in this paper: IRF, IFN regulatory factor; IKK, I κ B kinase; TBK1, TANK-binding kinase 1; RIG-I, retinoic acid-inducible gene I; CARD, caspase recruitment domain; MDA5, melanoma differentiation associated gene 5; MEF, mouse embryonic fibroblast; poly(I:C), poly(rI); poly(rC); NS3/4A, nonstructural protein 3/4A; siRNA, small interfering RNA; NDV, Newcastle disease virus; VSV, vesicular stomatitis virus; EMCV, encephalomyocarditis virus; eIF4A, eukaryotic initiation factor 4A; SeV, Sendai virus; FADD, Fas-associated protein with death domain.

of RIG-I/MDA5-mediated signaling, suggesting its role in negative feedback.

Materials and Methods

Cells, DNA transfection, preparation of cell extracts, and luciferase assay

L929 cells were maintained in MEM with 5% FBS and penicillin/streptomycin. 293T cells, Huh7 cells, and mouse embryonic fibroblasts (MEFs) were maintained in DMEM with 10% FBS and penicillin/streptomycin. The transient transfection of the L929 and 293T cells was performed as described previously (14). The 293T cells in Fig. 1C, Huh7 and MEFs, were transfected by FuGENE6 (Roche). The stable transformants of the L929 cells were established by the transfection of a linearized empty vector (pEF-BOS) or an expression plasmid for RIG-I (pEF-flagRIG-Ifull), RIG-IC (pEF-flagRIG-IC), MDA5 (pEF-flagMDA5full), or LGP2 (pEF-

flagLGP2) with pCDM8neo, followed by selection with G418 (1 mg/ml). Virus infection, poly(rI):poly(rC) (poly(I:C)) transfection, and preparation of cell extracts were performed as reported previously (14). Luciferase assay was performed with a dual-luciferase reporter assay system (Promega). As the internal control for the dual-luciferase assay, pRL-TK (Promega) was used.

Plasmid constructs

p-55C1BLuc, p-55UAS_GLuc, p-55A2Luc, p-125Luc, pEFGal4/IRF-3, pEFGal4/IRF-7, pEF-flagRIG-I, pEF-flagRIG-IC, pEF-flagRIG-IKA, pEF-flagIF4A, pcDNA3.1-nonstructural protein 3/4A (NS3/4A), pKS336-Sv-V, and pKS336-Sv-Vu were described previously (14, 18, 19). The pEF-flagRIG-IN, which contains the N-terminal 229 aa of RIG-I, was obtained by the insertion of oligonucleotides at the *EcoRI* sites of RIG-I cDNA. The cDNA of MDA5 was isolated by the RT-PCR technique, and inserted into the *XbaI/ClaI* sites of pEF-BOS⁺ with oligonucleotides for

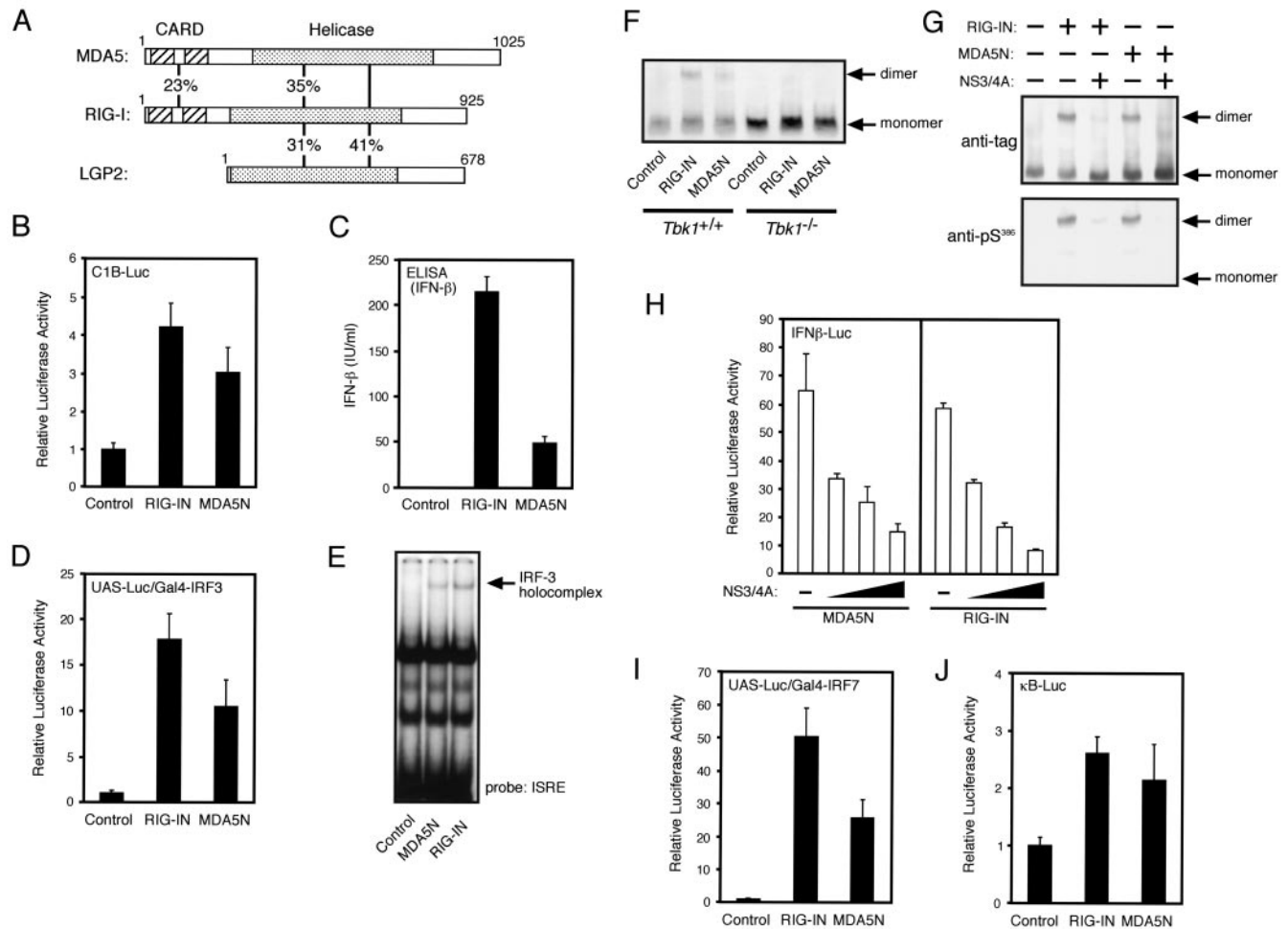


FIGURE 1. CARDs of RIG-I and MDA5 participate in a common signaling cascade. *A*, Schematic representation of RIG-I family helicases. Amino acid identities in the CARD and helicase domain are shown. *B*, L929 cells were transiently transfected with reporter constructs containing repeated IRF binding sites (p-55C1BLuc; C1B-Luc) together with the empty vector pEF-BOS (control), the RIG-IN expression construct (RIG-IN), or the MDA5N construct (MDA5N). At 48 h after transfection, the cells were subjected to the dual-luciferase assay. The relative firefly luciferase activity, normalized by the *Renilla* luciferase activity, is shown. Error bars show the SDs of triplicate transfections. *C*, 293T cells were transfected with a control vector, RIG-IN, or MDA5N. At 24 h after transfection, the IFN- β in the culture medium was quantified by ELISA. *D*, L929 cells were transfected with p-55UAS_GLuc and pEFGal4/IRF-3 together with pEF-BOS (control), RIG-IN, or MDA5N vector. Luciferase activity was normalized by the internal control pRL-TK. Error bars represent the SDs of triplicate transfections. *E*, The DNA-binding activity of the IRF-3-containing holocomplex was detected by EMSA using the ³²P-labeled IFN-stimulated response element oligonucleotide of the *isg15* gene as probe. The extract was prepared from the 293T cells that were transiently transfected with the indicated plasmids. *F*, The MEF cells prepared from *tbk1*^{+/+} or *tbk1*^{-/-} mice were transiently transfected with p50-tagged human IRF-3 along with the control vector, RIG-IN, or MDA5N plasmid. Extracts were subjected to native-PAGE, and the transfected IRF-3 was visualized by immunoblotting using an anti-p50 antiserum. *G*, 293T cells were transfected with p50-tagged IRF-3 together with the indicated plasmids. Extracts were subjected to native-PAGE followed by immunoblotting using an anti-p50 Ab (upper panel) and an anti-phosphoSer³⁸⁶ antiserum (lower panel). *H*, Huh7 cells were cotransfected with plasmids encoding the IFN- β luciferase reporter construct, *Renilla* luciferase, and MDA5N or RIG-IN vector with increasing amounts (0, 50, 100, and 200 ng) of the plasmid encoding NS3/4A (hepatitis C virus 1a), and subjected to luciferase assay. *I*, Reporter assay was performed as shown in *D*, except that pEFGal4/IRF-7 was used as effector. *J*, Reporter assay as in *B*, except that the NF- κ B reporter plasmid (p-55A2Luc) was used.

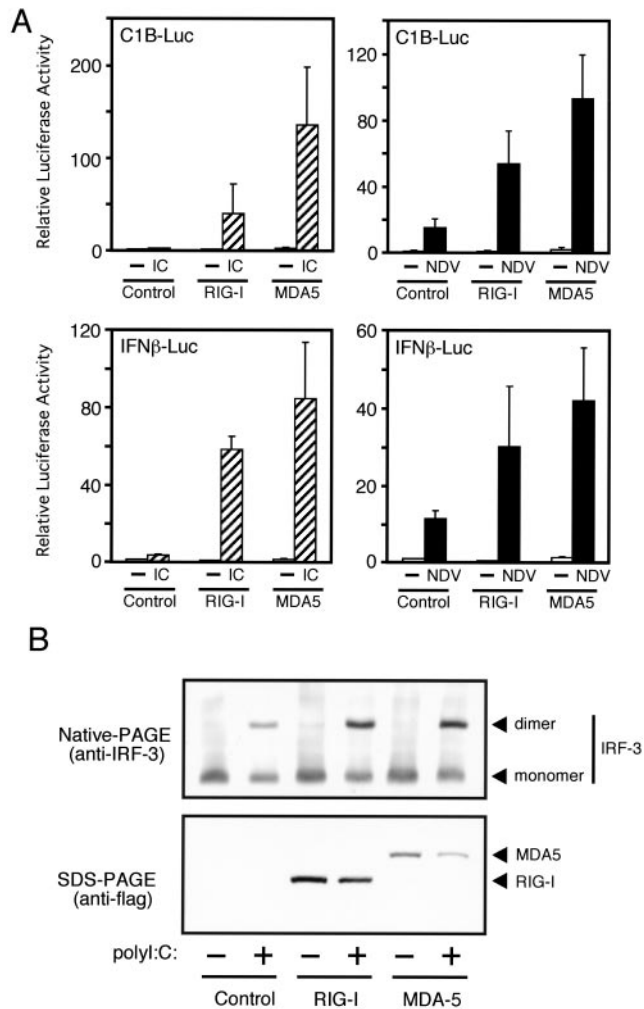


FIGURE 2. Stimulation-dependent activation of full-length RIG-I and MDA5. *A*, L929 cells were transfected with p-55C1BLuc (C1B-Luc) or the natural IFN- β gene promoter (p-125Luc; IFN β -Luc) together with pEF-BOS (control), full-length RIG-I, or MDA5. After stimulation with poly(I:C) transfection (6 h) or NDV infection (12 h), the cells were subjected to dual-luciferase assay. The relative firefly luciferase activity normalized by the *Renilla* luciferase activity is shown. Error bars show the SDs of triplicate transfections. *B*, L929-derived stable transformants expressing the *neo* gene alone (control) or flag-RIG-I or flag-MDA5 were stimulated with poly(I:C) transfection for 4 h. Endogenous IRF-3 was visualized by native-PAGE/immunoblotting using an anti-mouse IRF-3 antiserum (upper panel). The expressed RIG-I and MDA5 were detected by SDS-PAGE/immunoblotting using an anti-flag Ab (lower panel).

the N-terminal flag tag (pEF-flagMDA5). The nucleotide sequence of the cDNA was confirmed with a BigDye DNA-sequencing kit (Applied Biosystems). The cDNA of LGP2 (GenBank accession no. AK021416) was purchased from the Biological Resource Center of National Institute of Technology and Evaluation, and inserted into the *Xba*I sites of pEF-BOS with oligonucleotides for the N-terminal flag tag (pEF-flagLGP2). The deleted and site-directed mutants of MDA5 were obtained by the insertion of the appropriate oligonucleotides and the Kunkel method (20), respectively (pEF-flagMDA5N, pEF-flagMDA5C, and pEF-flagMDA5KA).

EMSA

EMSA was performed as described previously (14).

Abs, ELISA, immunoprecipitation, and immunoblotting

Anti-murine IRF-3, anti-p50-tag, and anti-V protein Abs were described in our previous reports (14, 19). The anti-flag (M2; Sigma-Aldrich) Ab and anti-actin Ab (Chemicon) are commercial products. The anti-LGP2 antiserum was obtained by immunizing the rabbits with synthetic peptides

(IQAKKWSRVPFVVC) of LGP2 conjugated to bovine thyroglobulin. The Ab was affinity-purified by using immobilized Ag peptide. We confirmed that this anti-LGP2 antiserum specifically recognized recombinant LGP2 expressed in 293T cells. ELISA, SDS-PAGE, native-PAGE, and immunoblotting were performed as described previously (14). Immunoprecipitation was performed as shown in previous report using anti-flag M2 affinity gel (Sigma-Aldrich) (5).

Poly(I:C)-pull-down assay

Poly(I:C)-pull-down assay was performed as described previously (14).

RNA interference

The vector for small interfering RNA (siRNA), piGENE hU6, and constructs for control or RIG-I siRNA were described previously (14). The sequences for the siRNA targeting murine MDA5 and LGP2 mRNA are 5'-GTCATTAGTAAATTTGCGACT-3' and 5'-GGATGGAGTTGGAA-GATGA-3', respectively. For the reporter assay, the L929 cells were transiently transfected with p-55C1BLuc and pRL-TK as reporters, together with the siRNA vectors. The cells were mock-infected or Newcastle disease virus (NDV)-infected, and subjected to dual-luciferase assay. The quantitative assay for endogenous mRNA was performed as described previously (14).

Virus yield titration

Stable L929-derived transformants were mock-infected or infected with vesicular stomatitis virus (VSV) or encephalomyocarditis virus (EMCV). The virus yield in culture supernatants was determined by plaque assay as described previously (14).

Mouse IFN titration

MEFs were stimulated by NDV infection or poly(I:C)/DEAE dextran transfection. After 24 h, culture media were collected, ultracentrifuged to remove viruses and poly(I:C) ($436,000 \times g$, 10 min), and subjected to IFN assay. The mouse IFN was titrated using the L929 cells in a 96-well plate and EMCV as a challenge virus. The IFN titer was normalized using an international standard.

Results

CARDs of RIG-I and MDA5 participate in a common signaling cascade

RIG-I and MDA5 share a limited homology in their overall primary structure (Fig. 1A). Notably, the two proteins contain tandem CARD-like regions at their N-termini as well as C-terminal DEXD/H-box helicase domains. The previous observation that the CARD of RIG-I and those of Nod1 and Nod2 target a distinct set of downstream molecules (14) prompted us to compare the functions of the CARDs of RIG-I and MDA5. The overexpression of the CARD of either RIG-I (RIG-IN) or MDA5 (MDA5N) resulted in the constitutive activation of the reporter p-55C1BLuc, which is essentially regulated by multimerized IRF binding sites (Fig. 1B). Furthermore, these CARDs activated the endogenous IFN- β gene, resulting in the secretion of the IFN- β protein without exogenous stimuli, such as viral infection (Fig. 1C). The fusion transcription factor containing the DNA-binding domain of Gal4 and the C-terminal regulatory domain of IRF-3 (Gal4-IRF-3) was activated by the expression of RIG-IN or MDA5N (Fig. 1D), showing that IRF-3 is a downstream target. Consistent with this, RIG-IN and MDA5N induced the IRF-3 holocomplex (Fig. 1E) and IRF-3 dimer (Fig. 1F). These results show that the CARD of MDA5 is capable of activating IRF-3 similarly to that of RIG-I. Interestingly, *tbk1*^{-/-} cells are defective in IRF-3 dimer formation induced by RIG-IN or MDA5N, suggesting that these CARDs signal through the protein kinase TBK1 (Fig. 1F). This is consistent with our observation that RIG-IN and MDA5N result in the phosphorylation of Ser 386 of IRF-3 (6) (Fig. 1G). It has been reported that the NS3/4A of the hepatitis C virus blocks RIG-I-mediated signaling through its protease activity (18). Although the target of the NS3/4A protease has not yet been identified, this hypothetical molecule functions downstream of MDA5N and RIG-IN, because the

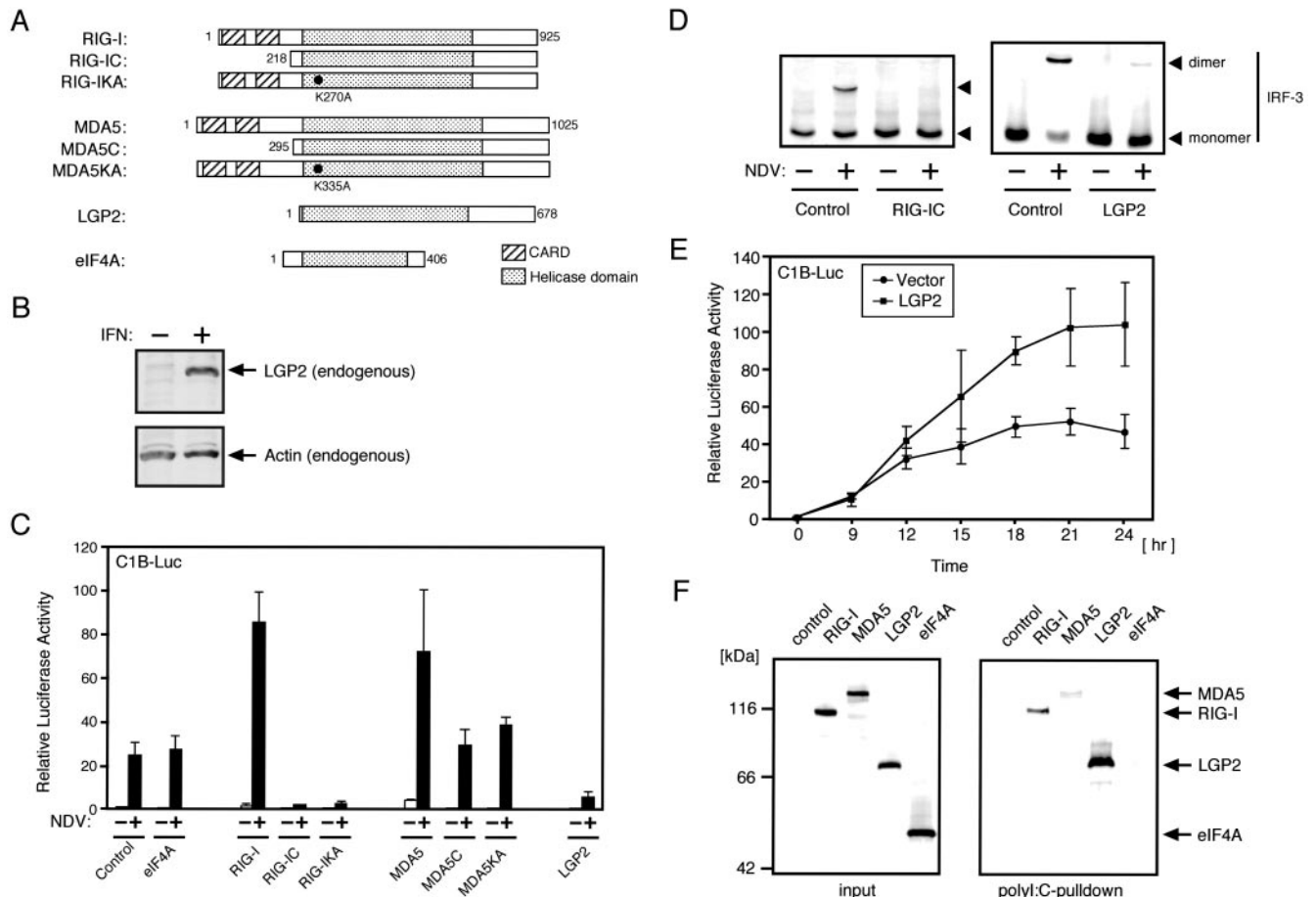


FIGURE 3. Functional analysis of RIG-I family proteins. *A*, Schematic representation of full-length and mutant helicases. *B*, L929 cells were cultured with a control medium (–) or a medium containing recombinant mouse IFN- β (+, 1000 IU/ml) for 12 h. Endogenous LGP2 and actin were detected by immunoblotting using an anti-LGP2 antiserum and anti-actin Ab, respectively. *C*, L929 cells were transfected with p-55C1BLuc (C1B-Luc) together with the indicated constructs. After stimulation with NDV infection (12 h), the cells were subjected to dual-luciferase assay. The relative firefly luciferase activity, normalized by the *Renilla* luciferase activity, is shown. Error bars show the SDs of triplicate transfections. *D*, L929-derived stable transformants expressing RIG-IC or LGP2 were stimulated with NDV for 9 h. Endogenous IRF-3 was separated by native PAGE and detected by immunoblotting using an anti-mouse IRF-3 antiserum. The positions of monomeric IRF-3 and dimeric IRF-3 are indicated. *E*, Knockdown of LGP2 expression by siRNA. L929 cells (5×10^5) were cotransfected with the reporter genes (250 ng of p-55C1BLuc and 10 ng of pRL-TK) and empty vector (vector, 2.5 μ g) or vector for siRNA targeting LGP2 (LGP2, 2.5 μ g). Cells were infected with NDV and subjected to dual-luciferase assay at the indicated time. Error bars show SD of triplicate transfections. *F*, Flag-tagged RIG-I, MDA5, LGP2, and eIF4A were produced in 293T cells, precipitated with poly(I:C)-agarose, and detected by immunoblotting using an anti-flag Ab (*right panel*). One-thirtieth of each extract used for pull-down assay was similarly separated and detected (*left panel*).

activation of IRF-3 was blocked by NS3/4A (Fig. 1, *G* and *H*). Moreover, Gal4-IRF-7 and NF- κ B were activated by RIG-IN and MDA5N (Fig. 1, *I* and *J*). In summary, these results strongly suggest that the CARDs of RIG-I and MDA5 activate the overlapping cascade.

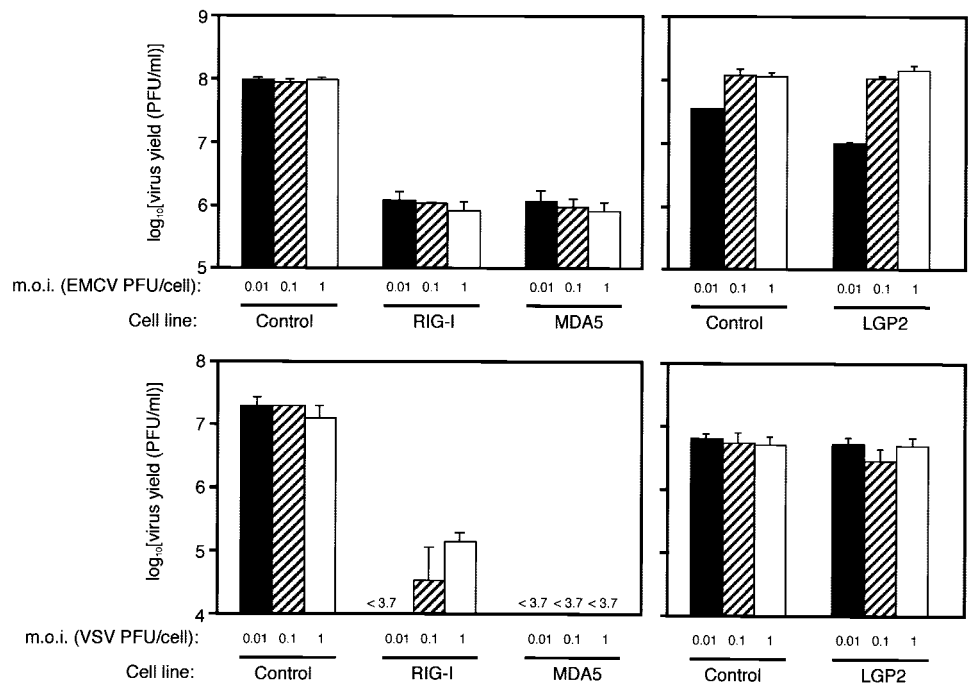
Positive and negative signalings by the full-length RIG-I, MDA5, and LGP2

The overexpression of the full-length RIG-I and MDA5 failed to activate the reporter genes, p-55C1BLuc and pIFN β Luc; however, considerable activation was observed after stimulation by virus infection or dsRNA transfection (Fig. 2*A*). Similarly, the dimerization of IRF-3 induced by dsRNA was increased by the overexpression of RIG-I or MDA5 without significant basal activation (Fig. 2*B*). These results show that RIG-I and MDA5 act as positive regulators of virus-induced signaling and are under strict negative regulation in the absence of stimuli.

The database search revealed another DExD/H-box helicase, LGP2, related to RIG-I and MDA5, but lacking CARD (Figs. 1*A*

and 3*A*). The LGP2 protein is markedly inducible by IFN- β , similarly to RIG-I and MDA5 (14, 21), whereas the house keeping actin expression was unaffected (Fig. 3*B*). To explore the functions of these proteins, we generated mutants of RIG-I and MDA5 lacking CARD (RIG-IC and MDA5C) as well as having an inactivated Walker's ATP binding motif by the Lys-to-Arg substitution of the respective helicases (RIG-IKA and MDA5KA). For comparison, a distantly related DExD/H helicase, eukaryotic initiation factor 4A (eIF4A), was used. Under these conditions, full-length RIG-I and MDA5 enhanced the virus-induced gene induction (Fig. 3*C*). eIF4A did not affect the virus-induced activation of the reporter; however, as reported earlier, RIG-IC and RIG-IKA strongly inhibited the virus-induced gene activation (14). In contrast, MDA5C and MDA5KA neither augmented nor suppressed the gene activation by the virus. In either case, the helicase domain alone is incapable of transducing positive signaling. Moreover, the results show that ATPase activity is critical to the functioning of RIG-I and MDA5 as positive regulators. LGP2 strongly inhibited the gene activation, similarly to RIG-IC. In cells stably expressing

FIGURE 4. Antiviral activities of RIG-I and MDA5. L929-derived stable transformants expressing RIG-I, MDA5, or LGP2 were infected with EMCV (*upper panel*) or VSV (*lower panel*) at the indicated multiplicity of infection (m.o.i.). After 24 h of infection, virus yield in the supernatant was determined by plaque assay.



RIG-IC or LGP2, virus-induced dimerization of endogenous IRF-3 was severely impaired (Fig. 3D). These results suggest that LGP2 functions as a physiological negative feedback regulator. Consistent with this, knockdown of LGP2 markedly enhanced gene activation induced by NDV infection (Fig. 3E). The binding of these helicases to dsRNA was investigated by pull-down assay (Fig. 3F). All of the tested helicases bound to poly(I:C)-agarose, except eIF4A with a relative affinity of LGP2 \gg RIG-I $>$ MDA5, confirming that the RIG-I family recognizes dsRNA.

Suppression of viral yield by RIG-I and MDA5

In our previous work, we showed that the stable expression of the RIG-I protein in cultured cells severely inhibits viral replication (14). We compared the antiviral activity of the RIG-I family by the same assay using EMCV and VSV as infecting viruses (Fig. 4). These viruses cause a severe “shutoff” of the host RNA and protein syntheses; thus, they are fully competent to induce lytic infection in L929 cells. RIG-I and MDA5 significantly reduced the viral yield 100- to 1000-fold, whereas LGP2 did not affect the viral yield. Likewise, the artificial inhibitor RIG-IC did not affect the viral yield (our unpublished observations).

Effect of inhibition of RIG-I and MDA5 on signal transduction

The above-mentioned results using mutant proteins indicate that, in addition to their structural homology, RIG-I and MDA5 share functional similarities. To explore the loss-of-function phenotype of these proteins, we performed knockdown of RIG-I and MDA5 using siRNA. We used luciferase reporter (Fig. 5A) and quantification of endogenous target gene expression (Fig. 5B) as readout. Vector and control siRNAs did not affect the virus-induced activation of the reporter p-55C1BLuc and endogenous IFN gene expression. The siRNA targeting endogenous mouse RIG-I or MDA5 blocked the gene induction in a dose-dependent manner (Fig. 5A). Furthermore, the expression of endogenous IFN mRNA was specifically inhibited by siRNA for either RIG-I or MDA5 (Fig. 5B). These results indicate the requirement of endogenous RIG-I and MDA5 in the signaling.

Recently, a report has shown that V proteins encoded by paramyxoviruses inhibit the MDA5-induced activation of type I

IFN genes (16). The inhibition is apparently mediated by the direct association between V proteins and MDA5. We investigated the effect of the Sendai virus (SeV) V protein on signaling by RIG-I and MDA5 (Fig. 6A). We used an expression vector for the entire coding region of the V protein (sharing the N-terminal 316 aa with the P protein: 384 aa) and a partial clone encompassing the C-terminal region unique to the V protein (Vu: 68 aa). The expression of the SeV V protein caused a marginal (~30%) suppression of the NDV-induced reporter gene expression, suggesting that the NDV-induced signal is largely insensitive to the V-protein-mediated inhibition. The expression of RIG-I resulted in a marked augmentation of the NDV-induced reporter gene activation; however, it was not notably affected by the V protein expression. In contrast, the enhancement of the virus-induced gene activation by MDA5 was completely abrogated by the V protein as reported (16). A Vu protein exhibited an activity indistinguishable from that of the V protein, indicating that the C-terminal region is sufficient for the inhibition. The selective inhibition of MDA5 by V protein is likely due to selective physical interaction as revealed by co-precipitation experiment (Fig. 6B), in which RIG-I did not interact with V protein.

Recently, Balachandran et al. (22) have reported that Fas-associated protein with death domain (FADD) plays an essential role in the poly(I:C)-induced induction of type I IFN genes as well as in apoptosis. We used fibroblasts derived from wild-type and knockout mice for *irf-3*, *tbk1*, and *fadd* genes. These cells were either infected with NDV or transfected with poly(I:C) by the DEAE dextran method, and the secreted IFN was quantified (Table I). The wild-type cells efficiently produced IFN after NDV infection; however, this production was markedly reduced in cells deficient in IRF-3 and TBK1, consistent with previous reports (4, 10, 11, 23). FADD-deficient cells produced IFN at a level comparable to that of the wild-type cells, showing that FADD is not necessary in the signaling by NDV. However, when these cells were transfected with poly(I:C), FADD was observed to be apparently necessary for the IFN production along with other signaling components such as IRF-3 and TBK1. This result shows that virus and a synthetic dsRNA trigger the partially shared but distinct signaling cascade.

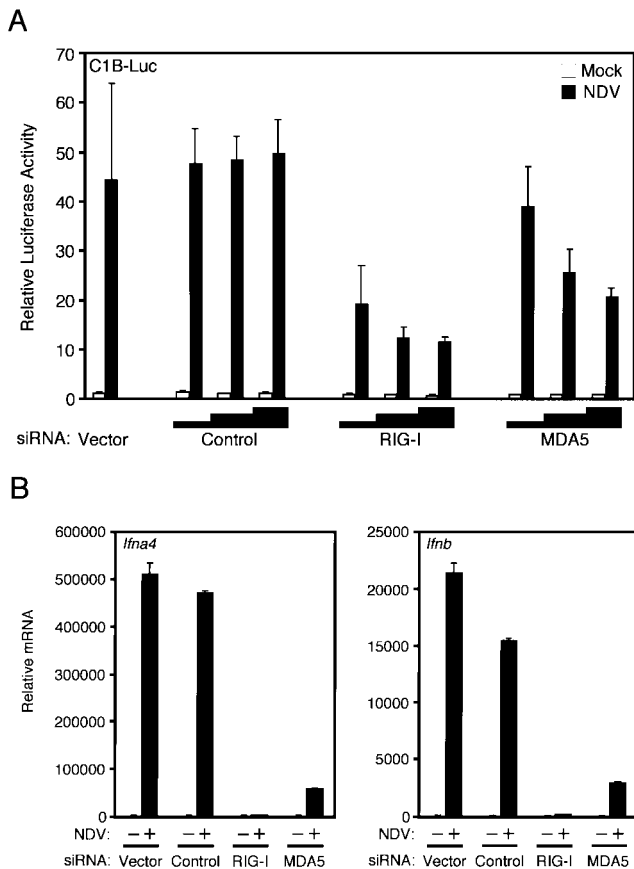


FIGURE 5. Knockdown of RIG-I and MDA5 expression by siRNA. *A*, L929 cells (2×10^5) were cotransfected with the reporter genes (200 ng of p-55C1BLuc and 4 ng of pRL-TK) and increasing amounts of vectors for siRNA (400, 600, and 800 ng). The cells were mock-infected or NDV-infected for 12 h, and subjected to dual-luciferase assay. Error bars show the SDs of triplicate transfections. *B*, L929 cells were transfected with the indicated siRNA vectors together with the plasmid for puromycin-resistant gene. After cultivation in the presence of puromycin (10 μ g/ml) for 3 days, cells were mock-infected or NDV-infected for 12 h. Total RNA was prepared, and subjected to real-time PCR using the primer-probe sets for mouse *IFN- α 4* and *IFN- β* genes.

Discussion

In the present report, we show that RIG-I and MDA5 participate in the viral induction of a type I IFN system. The CARDs of these proteins mediate downstream signaling. However, full-length proteins remain inactive, possibly due to intramolecular inhibition by the helicase domain. This inhibition is reversed by cytoplasmic dsRNA by interacting with the helicase domain, followed by the activation of its ATPase activity, although the precise mechanism remains to be clarified. Both RIG-I and MDA5 activate a pathway sensitive to viral NS3/4A, resulting in the activation of IRF-3 and NF- κ B. We do not know the direct target of RIG-I and MDA5 at present. FADD is unlikely the hypothetical target because it is dispensable in the signaling triggered by NDV. Its requirement in poly(I:C)-induced signaling suggests its role during or after the cytoplasmic uptake of extracellular dsRNA.

The following observations suggest that RIG-I and MDA5 function in parallel rather than in series. First, the knockdown of either proteins partially blocked the signaling (Fig. 5). Second, the SeV V protein, which is a potent and selective inhibitor of MDA5, did not completely abrogate the signaling (Fig. 6). Third, the expression of RIG-I and MDA5 did not exhibit a marked synergy in reporter assays (our unpublished observations). Finally, the *Fugu*

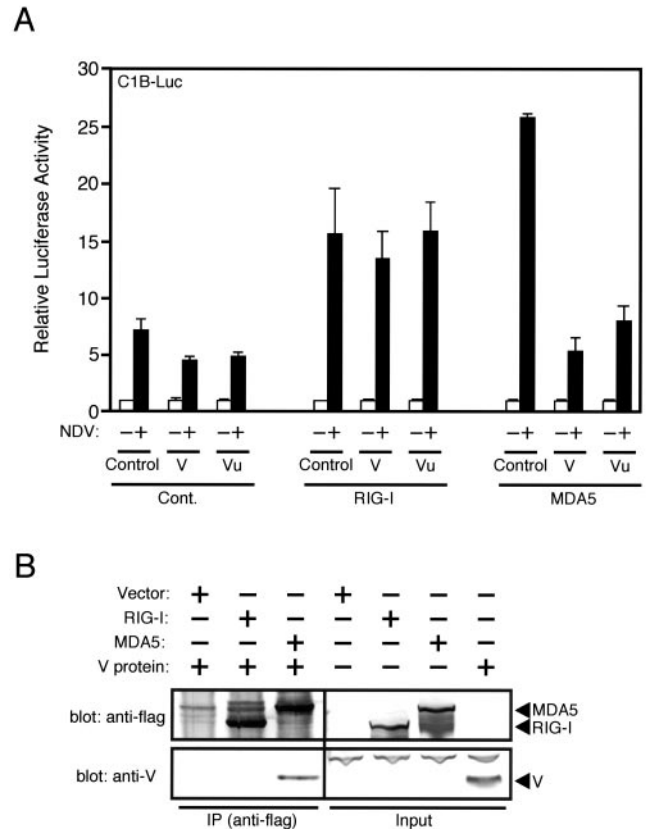


FIGURE 6. The V protein of SeV selectively inhibited MDA5-mediated signaling. *A*, L929 cells were transfected with reporter constructs (p-55C1BLuc and pRL-TK) along with the indicated combination of expression vectors. Cells were mock-infected or NDV-infected for 12 h. The relative firefly luciferase activity normalized by the *Renilla* luciferase activity is shown. *B*, 293T cells were transfected with empty vector (pEF-BOS), flag-tagged full-length RIG-I, flag-tagged full-length MDA5, or SeV V protein vectors. Expression of the proteins was confirmed by immunoblotting using anti-flag or anti-V protein Abs (input). The indicated extracts were mixed on ice for 10 min and subjected to immunoprecipitation (IP) using anti-flag M2 Gel (Sigma-Aldrich). The precipitated RIG-I, MDA5, and V protein were detected by immunoblotting.

genome contains a single gene encoding the CARD-containing helicase related to RIG-I and MDA5. RIG-I and MDA5 are ubiquitously expressed in various mouse tissues, except in the brain and spinal cord (24). Our analyses revealed that these proteins function similarly, except some details. Overexpression of CARD of RIG-I activated endogenous IFN- β gene more efficiently than that of MDA5 (Fig. 1C), although these proteins activated IRF-3, IRF-7, and NF- κ B efficiently (Fig. 1). Therefore, we do not exclude a possibility of differential activation of unidentified transcription factor(s) by RIG-I and MDA5. A more clear distinction between these proteins is selective inhibition of MDA5 by V protein, due to specific physical interaction (Fig. 6). Thus, having two

Table I. *IFN* production by MEFs of different genotypes

Genotype	IFN Production (IU/ml)	
	NDV	Poly(I:C)/DEAE Dextran
<i>irf-3</i> ^{+/+}	5120	160
<i>irf-3</i> ^{-/-}	80	<20
<i>tbk1</i> ^{-/-}	160	<20
<i>fadd</i> ^{-/-}	5120	<20

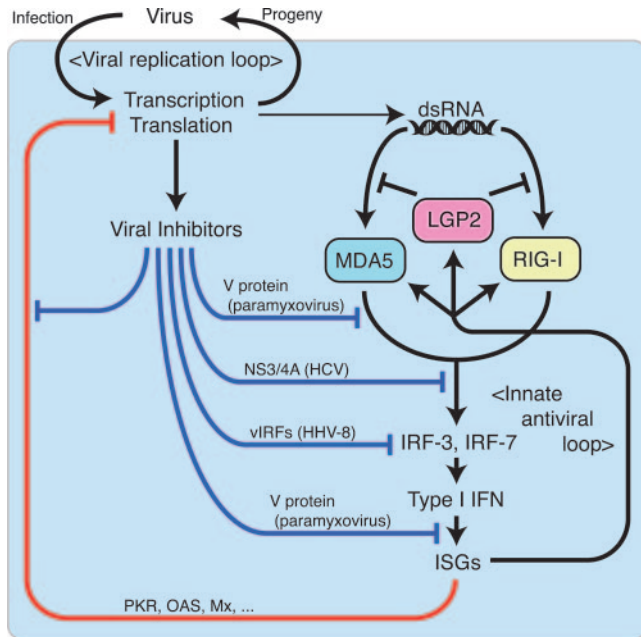


FIGURE 7. Innate antiviral loop and virus replication loop. When viruses, particularly RNA viruses, infect cells, its genome starts to replicate and express encoded genes. Genome replication results in dsRNA, which is recognized by the sensor molecules RIG-I and MDA5. These sensors transmit signals to activate downstream cascades, including the activation of transcription factors (IRF-3, -7), IFN genes, IFN-induced signaling, and IFN-inducible genes (IFN-stimulated genes (ISGs)). Because RIG-I and MDA5 are IFN-inducible, this activation loop undergoes amplification. Another IFN-inducible helicase, LGP2, acts as a negative regulator for the loop. A group of ISGs encode antiviral proteins, which directly inhibit viral replication (red line). Viruses encode a number of proteins inhibiting the innate antiviral loop (blue lines). These two loops are mutually inhibitory. PKR, dsRNA-dependent protein kinase; OAS, 2'-5' oligoadenylate synthetase; HHV, human herpes virus.

genes with overlapping functions may be beneficial in avoiding the viral inhibitors.

In cytokine signaling, negative regulators have been identified, which provide a negative feedback loop for avoiding uncontrolled signaling (25). Defects in these negative regulators often result in pathological conditions due to excessive reaction. LGP2 belongs to the RIG-I family, but lacks CARD. Similarly to the artificial RIG-IC and RIG-IKA, LGP2 acts as a strong inhibitor of virus-induced signaling, whereas MDA5C and MDA5KA do not. The observations that MDA5 binds to dsRNA with a lower affinity than RIG-I and LGP2 (Fig. 3F), and that RIG-IC and LGP2 are incapable of blocking the signaling induced by the overexpression of RIG-IN (our unpublished observations), indicate that the sequestration of dsRNA from wild-type RIG-I and MDA5 is the mechanism of the inhibition. It is worth noting that, although the binding affinity of MDA5 is significantly low, MDA5 efficiently transmits signals by poly(I:C) (Fig. 2A), suggesting that the binding affinity per se does not determine downstream signaling. Therefore, it is tempting to speculate that transient formation of MDA5/dsRNA complex is sufficient to trigger downstream signaling ("hit-and-run model"), however to inhibit the signaling, persistent "sequestration" by stable complex formation is required. Alternatively, involvement of additional regulatory factor(s) in the recognition of dsRNA by RIG-I and MDA5 is a possibility. Interestingly, proteins with unrelated dsRNA binding motifs, including a dsRNA-dependent protein kinase, an RNA-specific adenosine deaminase, and a protein activator of dsRNA-dependent protein

kinase, do not inhibit the virus-induced signaling (26), suggesting that LGP2 specifically masks the target RNA from recognition by RIG-I and MDA5. LGP2 is strongly induced by type I IFN (Fig. 3B), and knockdown of LGP2 results in enhanced gene induction (Fig. 3E); thus, it is likely responsible for the negative feedback of IFN gene activation.

Figure 7 shows the signaling cascade triggered by virus infection. Because RIG-I and MDA5 are IFN-inducible (14, 21), once the signal is triggered by the virus, this innate antiviral loop initiates autoamplification until the triggering molecule dsRNA is removed and/or the natural inhibitor LGP2 is induced. The viral genome also undergoes autoamplification through the expression of the viral proteins. Apparently, the two amplifications are mutually inhibitory through virus-encoded inhibitory peptides and host antiviral proteins. Particularly, an increasing number of studies suggest that viruses encode numerous inhibitory proteins for the molecules of the innate antiviral loop (27). In summary, the outcome of an infection is determined by the equilibrium between viral replication and innate antiviral responses, concretely by the viral load, the activities of viral inhibitors, and the host signaling molecules including RIG-I and MDA5. This principle may be useful in designing antiviral drugs and therapies. Particularly, the agonist of RIG-I and MDA5 is expected to enable the potentiation of host antiviral innate immunity.

Acknowledgments

We thank Drs. T. Taniguchi and G. Barber for providing *irf-3^{-/-}* and *fadd^{-/-}* MEFs, respectively.

Disclosures

The authors have no financial conflict of interest.

References

- De Maeyer, E., and J. De Maeyer-Guignard. 1998. Type I interferons. *Int. Rev. Immunol.* 17: 53–73.
- Samuel, C. E. 2001. Antiviral actions of interferons. *Clin. Microbiol. Rev.* 14: 778–809.
- Malmgaard, L. 2004. Induction and regulation of IFNs during viral infections. *J. Interferon Cytokine Res.* 24: 439–454.
- Sato, M., H. Suemori, N. Hata, M. Asagiri, K. Ogasawara, K. Nakao, T. Nakaya, M. Katsuki, S. Noguchi, N. Tanaka, and T. Taniguchi. 2000. Distinct and essential roles of transcription factors IRF-3 and IRF-7 in response to viruses for IFN- α gene induction. *Immunity* 13: 539–548.
- Yoneyama, M., W. Suhara, Y. Fukuhara, M. Fukuda, E. Nishida, and T. Fujita. 1998. Direct triggering of the type I interferon system by virus infection: activation of a transcription factor complex containing IRF-3 and CBP/p300. *EMBO J.* 17: 1087–1095.
- Mori, M., M. Yoneyama, T. Ito, K. Takahashi, F. Inagaki, and T. Fujita. 2004. Identification of Ser-386 of interferon regulatory factor 3 as critical target for inducible phosphorylation that determines activation. *J. Biol. Chem.* 279: 9698–9702.
- Fitzgerald, K. A., S. M. McWhirter, K. L. Faia, D. C. Rowe, E. Latz, D. T. Golenbock, A. J. Coyle, S. M. Liao, and T. Maniatis. 2003. IKK ϵ and TBK1 are essential components of the IRF3 signaling pathway. *Nat. Immunol.* 4: 491–496.
- Sharma, S., B. R. tenOever, N. Grandvaux, G. P. Zhou, R. Lin, and J. Hiscott. 2003. Triggering the interferon antiviral response through an IKK-related pathway. *Science* 300: 1148–1151.
- Yoneyama, M., W. Suhara, and T. Fujita. 2002. Control of IRF-3 activation by phosphorylation. *J. Interferon Cytokine Res.* 22: 73–76.
- Hemmi, H., O. Takeuchi, S. Sato, M. Yamamoto, T. Kaisho, H. Sanjo, T. Kawai, K. Hoshino, K. Takeda, and S. Akira. 2004. The roles of two I κ B kinase-related kinases in lipopolysaccharide and double stranded RNA signaling and viral infection. *J. Exp. Med.* 199: 1641–1650.
- Perry, A. K., E. K. Chow, J. B. Goodnough, W. C. Yeh, and G. Cheng. 2004. Differential requirement for TANK-binding kinase-1 in type I interferon responses to toll-like receptor activation and viral infection. *J. Exp. Med.* 199: 1651–1658.
- Marie, I., J. E. Durbin, and D. E. Levy. 1998. Differential viral induction of distinct interferon- α genes by positive feedback through interferon regulatory factor-7. *EMBO J.* 17: 6660–6669.
- Sato, M., N. Hata, M. Asagiri, T. Nakaya, T. Taniguchi, and N. Tanaka. 1998. Positive feedback regulation of type I IFN genes by the IFN-inducible transcription factor IRF-7. *FEBS Lett.* 441: 106–110.
- Yoneyama, M., M. Kikuchi, T. Natsukawa, N. Shinobu, T. Imaizumi, M. Miyagishi, K. Taira, S. Akira, and T. Fujita. 2004. The RNA helicase RIG-I

- has an essential function in double-stranded RNA-induced innate antiviral responses. *Nat. Immunol.* 5: 730–737.
15. Kang, D. C., R. V. Gopalkrishnan, Q. Wu, E. Jankowsky, A. M. Pyle, and P. B. Fisher. 2002. mda-5: an interferon-inducible putative RNA helicase with double-stranded RNA-dependent ATPase activity and melanoma growth-suppressive properties. *Proc. Natl. Acad. Sci. USA* 99: 637–642.
 16. Andrejeva, J., K. S. Childs, D. F. Young, T. S. Carlos, N. Stock, S. Goodbourn, and R. E. Randall. 2004. The V proteins of paramyxoviruses bind the IFN- β promoter. *Proc. Natl. Acad. Sci. USA* 101: 17264–17269.
 17. Miyoshi, K., Y. Cui, G. Riedlinger, P. Robinson, J. Lehoczy, L. Zon, T. Oka, K. Dewar, and L. Hennighausen. 2001. Structure of the mouse Stat 3/5 locus: evolution from *Drosophila* to zebrafish to mouse. *Genomics* 71: 150–155.
 18. Foy, E., K. Li, R. Sumpter, Jr., Y. M. Loo, C. L. Johnson, C. Wang, P. M. Fish, M. Yoneyama, T. Fujita, S. M. Lemon, and M. Gale, Jr. 2005. Control of antiviral defenses through hepatitis C virus disruption of retinoic acid-inducible gene-1 signaling. *Proc. Natl. Acad. Sci. USA* 102: 2986–2991.
 19. Kato, A., C. Cortese-Grogan, S. A. Moyer, F. Sugahara, T. Sakaguchi, T. Kubota, N. Otsuki, M. Kohase, M. Tashiro, and Y. Nagai. 2004. Characterization of the amino acid residues of Sendai virus C protein that are critically involved in its interferon antagonism and RNA synthesis down-regulation. *J. Virol.* 78: 7443–7454.
 20. Kunkel, T. A. 1985. Rapid and efficient site-specific mutagenesis without phenotypic selection. *Proc. Natl. Acad. Sci. USA* 82: 488–492.
 21. Kang, D. C., R. V. Gopalkrishnan, L. Lin, A. Randolph, K. Valerie, S. Pestka, and P. B. Fisher. 2004. Expression analysis and genomic characterization of human melanoma differentiation associated gene-5, mda-5: a novel type I interferon-responsive apoptosis-inducing gene. *Oncogene* 23: 1789–1800.
 22. Balachandran, S., E. Thomas, and G. N. Barber. 2004. A FADD-dependent innate immune mechanism in mammalian cells. *Nature* 432: 401–405.
 23. McWhirter, S. M., K. A. Fitzgerald, J. Rosains, D. C. Rowe, D. T. Golenbock, and T. Maniatis. 2004. IFN-regulatory factor 3-dependent gene expression is defective in Tbk1-deficient mouse embryonic fibroblasts. *Proc. Natl. Acad. Sci. USA* 101: 233–238.
 24. Ida-Hosonuma, M., T. Iwasaki, T. Yoshikawa, N. Nagata, Y. Sato, T. Sata, M. Yoneyama, T. Fujita, C. Taya, H. Yonekawa, and S. Koike. 2005. The $\alpha\beta$ interferon response controls tissue tropism and pathogenicity of poliovirus. *J. Virol.* 79: 4460–4469.
 25. Yoshimura, A., H. Mori, M. Ohishi, D. Aki, and T. Hanada. 2003. Negative regulation of cytokine signaling influences inflammation. *Curr. Opin. Immunol.* 15: 704–708.
 26. Iwamura, T., M. Yoneyama, N. Koizumi, Y. Okabe, H. Namiki, C. E. Samuel, and T. Fujita. 2001. PACT, a double-stranded RNA binding protein acts as a positive regulator for type I interferon gene induced by Newcastle disease virus. *Biochem. Biophys. Res. Commun.* 282: 515–523.
 27. Sen, G. C. 2001. Viruses and interferons. *Annu. Rev. Microbiol.* 55: 255–281.